Effects of Non-Maxwellian Electron Velocity Distributions on Parametric Instabilities

B. B. Afeyan*
A. E. Chou**
W. L. Kruer

Introduction

It is well known that non-Maxwellian electron velocity distribution functions (VDFs) exist in plasmas where there are sources of energy to sustain the plasma state away from the usual Maxwellian equilibrium. Whether it be nonlinear many-wave interactions, such as described by quasilinear theory for example[1]; turbulence,[2] a high-power laser heating a high-Z plasma,[3–7] or nonlocal heat transport in laser-produced plasmas due to steep temperature gradients,[8,9] non-Maxwellian velocity distributions have long been identified for conditions that are readily accessible in experiments today. A concrete example in laser-produced plasmas occurs when a strong enough laser irradiates a target such that the ionization state Z multiplied by the ratio of the oscillatory energy of the electrons in the field of the laser divided by their thermal energy in the plasma is 0.1. Dum[2] proposed a family of super-Gaussian distribution functions that can continuously vary from a Maxwellian ($n = 2$) to the saturated ($n = 5$) limit later explored in laser plasmas by Langdon and others.[3–7] In the latter context, when the laser intensity is sufficiently high, electron–ion heating takes place fast enough that electron–electron collisions cannot equilibrate the distribution, giving rise to these novel states. Fokker–Planck simulations have shown that such non-Maxwellian distribution functions retain their shape even in the presence of heat transport and other gradient-driven processes in the plasma.[6,7]

An important area of current research in inertial confinement fusion is the study of high-temperature hohlraums,[10] which have smaller dimensions than scale 1 hohlraums typically used on Nova.[11] These Au hohlraums do not contain fill gases, and the laser intensities used are in the 10^{16}-W/cm^2 or higher range. Clearly, such conditions are ripe for the development of non-Maxwellian distributions in the Au plasma. In addition, the importance of non-Maxwellians has been recently reinforced in two sets of Nova experiments[12,13] that used high-Z plasmas to study the behavior of parametric instabilities[14–16,11] such as stimulated Raman scattering (SRS)—the decay of an electromagnetic wave (EMW) into an electron–plasma wave (EPW) and a scattered EMW—and stimulated Brillouin scattering (SBS)—the decay of an EMW into a scattered EMW and an ion-acoustic wave (IAW). These experiments recorded the reflected levels of SRS and SBS as a function of the fractional composition of a low-Z dopant in the high-Z, Xe plasma. The data show that ion-wave properties do indeed affect SRS reflectivities via modifications of the levels of secondary instabilities.[12,13,17]

All such arguments, however, in order to be made quantitative, require that we know the frequencies and damping rates of their constituent EPWs, EMWs, and IAWs. Secondary instabilities such as the Langmuir decay[18–20] (LDI, the decay of an EPW into another EPW and an IAW) and the electromagnetic decay[21] (EDI, the decay of an EPW into an EMW and an IAW) instabilities have been studied in the past but only under the assumption that the velocity distribution of the electrons is a Maxwellian. Our results indicate that in the Xe experiments,[12,13] LDI has a threshold comparable to that of EDI and not the much higher one that Maxwellian Landau damping would have implied.

In this article, we present the results of the first systematic and not-just-perturbative calculation of the solutions of the plasma-dispersion relation in Dum-Langdon-Matte (DLM) distribution functions.[2,3,6] These are super-Gaussians whose exponents range from 2 to 5. Previous attempts to address EPWs in DLM

*   University of California at Davis, Davis, CA.
** University of California at Los Angeles, Los Angeles, CA.

distributions relied on first-order perturbation-theory evaluation of the damping rate, which our results (see Figure 1) show to be insufficiently accurate for the tasks at hand.[22–24] We also treat IAWs in DLM electron and Maxwellian ion VDFs for the first time and find novel changes in the behavior of IAWs. Strictly Maxwellian models have been routinely used to solve the kinetic dispersion relations for SRS and SBS,[26,27,11] sometimes including laser hot-spot models and additional Maxwellian hot-electron tails in an attempt to bridge the gap between theory and experiment.[24,28,29] We have developed a dispersion relation solver that calculates the Hilbert transform of any differentiable isotropic distribution function. We restrict our attention here to DLM VDFs because they provide an adequate description of smooth transitions from a Maxwellian to flat-top/depleted-tail VDFs as the laser intensity is increased in a moderate- to high-Z plasma.

This article states the plasma dispersion relations to be solved, sketches the solution method, and then shows the frequencies and damping rates of EPWs and IAWs as a function of wave-number and super-Gaussian exponent n. In addition, we use a result obtained via the Fokker–Planck simulations of Matte[5,6] (which is an empirical formula relating plasma temperature, ionization state, and laser intensity and wavelength to a given n super-Gaussian distribution function) to show damping rates of EPWs as functions of these physical parameters. This is strictly a conservative estimate of what would happen in a spatially nonuniform intensity distribution. An RPP (random phase plate)[25] laser model is adopted next and the gain of SRS calculated vs angle for different Z values. We observe that within a hot spot, not only will the laser intensity be higher than average, but the intensity-dependent damping rate of EPWs will be lower as well, making the spatial gain of the instability very much larger, as it is proportional to the exponential of the spatial integral of the ratio of these two quantities. Ramifications of these results for parametric instabilities in moderate- to high-Z plasmas are discussed, and a new model is put forward that seems to capture various seemingly unrelated trends in the many outstanding problems that exist in the interpretation of Raman and Brillouin backscattering experimental observations.

The Theoretical Model

The linear theory of parametric scattering instabilities taking into account kinetic effects was originally presented by Drake et al.[26,15] The dispersion relations to be solved for Raman and Brillouin, for instance, are

$$\frac{1}{\chi_e} + \frac{1}{1 + \sum_j \chi_i^{(j)}} = c^2 k^2 \frac{v_0^2}{4c^2}\left[\frac{|\hat{v}_0 \times k_-|^2}{k_-^2 D_-} + \frac{|\hat{v}_0 \times k_+|^2}{k_+^2 D_+}\right] \quad (1)$$

where the electron and ion susceptibilities are

$$\chi_{e,i} = \frac{\omega_{Pe,i}^2}{N_{0e,i} k^2} \int \frac{k \cdot \partial f_{0e,i}/\partial v}{(\omega - k \cdot v)} dv \quad (2)$$

and the electromagnetic Stokes (–) and anti-Stokes (+) sidebands have the following dispersion relations:

$$D_\pm = c^2(k \pm k_0)^2 - (\omega \pm \omega_0)^2$$
$$+ \omega_P^2[1 - i\bar{\nu}_{ei}/(\omega \pm \omega_0)]. \quad (3)$$

The DLM VDFs may be written in the form

$$f_{0e} = C(n)\frac{N_{e0}}{v_e^3} \exp\left[-\left(\frac{|v|}{\alpha_e v_e}\right)^n\right], \quad (4)$$

where v_e^2 is proportional to the electron temperature and the constant $\alpha_e = [3\Gamma(3/n)/\Gamma(5/n)]^{1/2}$ is chosen to ensure the proper definition of temperature in terms of the second moment of the 3D distribution function. The overall normalization factor is

$$C(n) = \left[1/\left(4\pi\alpha_e^3\right)\right]\left[n/\Gamma(3/n)\right],$$

chosen so that the zero-order moment of the 3D distribution function reduces to the density, N_{e0}. As the DLM exponent n is increased from the Maxwellian limit of $n = 2$ to the limit where electron–electron collisions are entirely negligible, $n = 5$, the distribution functions have increasingly more flattened cores and depleted tails. The waterbag model is reached in the limit $n \to \infty$. Matte[5,6] has obtained the connection between the exponent n and parameters that characterize the laser-plasma system in steady-state constant-intensity illumination simulations. With the laser intensity I defined in units of 10^{15} W/cm^2, laser wavelength λ_0 in units of 0.35 μm, and the electron temperature T_e in keV, the conversion is

$$\bar{Z}I_{15,W/cm^2}\lambda_{0,0.35\mu m}^2/T_{e,keV} = 44.29\left[(n-2)/(5-n)\right]^{1.381}.$$

The dispersion relation for an EPW in any isotropic VDF is obtained by neglecting the coupling

due to the pump as well as ignoring the (low-frequency) ion susceptibility contribution in Eq. (1):

$$\varepsilon = (1 + Ak^2\lambda_{De}^2) + \sqrt{\pi}\,\zeta_0 I(\zeta_0) = 0 \tag{5}$$

where the coefficient A describes the modified Debye shielding properties in non-Maxwellian electron VDFs. It renormalizes the temperature defined by the rule that the average kinetic energy be equal to $(3/2)kT_e$, giving rise to a new effective Debye shielding temperature boosted by this factor A. A is proportional to the ratio of the second to zeroth moments of the VDF:

$$A = \frac{n_{e0}}{2\hat{f}_e} \tag{6}$$

$$n_{e0} = 4\pi\int_0^\infty f_e(\xi)\,\xi^2\,d\xi \tag{7}$$

and

$$\hat{f}_e = \int_{-\infty}^\infty f_e(\xi)\,d\xi . \tag{8}$$

Here $\xi = v/v_{th}$, and the thermal velocity is given by

$$v_{th}^2 = (4\pi/3)\int_0^\infty v^4 f_e(v)\,dv . \tag{9}$$

The normalized phase velocity is $\zeta_0 = v_\phi/v_{th}$, while the function $I(\zeta_0)$ is defined in terms of an integral along a Landau contour:

$$I(\zeta_0) = \frac{1}{\sqrt{\pi}\,\hat{f}_e}\int_{LC}\frac{f_e(\xi)\,d\xi}{\xi - \zeta_0} . \tag{10}$$

These results are true for any isotropic VDF. Specializing to the case of DLMs, the energy to Debye shielding temperature renormalization factor, A, defined in Eqs. (6–8), becomes

$$A(n) = \frac{3\,\Gamma^2(3/n)}{\Gamma(1/n)\,\Gamma(5/n)} , \tag{11}$$

while the function I may be expressed as a principal value integral plus a simple pole contribution:

$$I(\zeta_0;n) = \frac{1}{\sqrt{\pi}}PV\int_{-\infty}^\infty d\xi\,\frac{\exp[-|\xi|^n]}{\xi - \zeta_0} + 2i\sqrt{\pi}\exp[-\zeta_0^n]$$

$$= I_R + iI_I + I_{pole} \tag{12}$$

$$I_R = \frac{1}{\sqrt{\pi}}\int_{-\infty}^\infty d\xi\,\frac{\xi - \Re(\zeta_0)}{(\xi - \Re(\zeta_0))^2 + (\Im(\zeta_0))^2}\exp[-|\xi|^n] \tag{13}$$

$$I_I = \frac{1}{\sqrt{\pi}}\int_{-\infty}^\infty d\xi\,\frac{\Im(\zeta_0)}{(\xi - \Re(\zeta_0))^2 + (\Im(\zeta_0))^2}\exp[-|\xi|^n] . \tag{14}$$

For DLMs, it is convenient to use $\zeta_0 = (\omega/\omega_p)/[\sqrt{2}(k\lambda_{De})]$ as the normalized phase velocity of an EPW. The root finder must solve Eq. 5 for ζ_0 given a value of $(k\lambda_{De})^2$. For $n = 2$, the function $I(\zeta_0, n)$ reduces to the Hilbert transform of a Gaussian, and is simply the plasma dispersion function $Z(\zeta_0)$.

For small $k\lambda_{De}$, the integrands in Eqs. (13) and (14) are sharply peaked at the pole location and therefore sensitive functions of $k\lambda_{De}$. This becomes more severe as n increases and the tails become more depleted. For example, in the case of the Maxwellian, the amplitude of the integrand in I_I at the pole varies by a factor of 4.4, as $k\lambda_{De}$ is varied from 0.3 to 0.55, whereas in the same range but for $n = 5$, I_I varies by four orders of magnitude. A strategy is required in order to avoid nonconvergence problems associated with finding zeros of functions defined implicitly via integrals with sensitive dependences on the independent variable.

One such method is to start with small values of k_{De}, such as 0.2, and the Maxwellian VDF. By using the analytic estimate for the root of the dispersion relation found by perturbation theory, one can use a Z-function evaluator to solve the dispersion relation instead of calculating the Hilbert transform integrals directly. Increasing values of k_{De} can be treated by using the roots at the previous value as a starting guess. Once a k_{De} of $O(1)$ is reached, the I function evaluator can be used to go to higher n in small increments. When the desired n is reached, one may redescend to smaller values of k_{De}, at that large n, using the latest root as a guess. With this procedure, one may study small k_{De} values for any n without uncontrolled error accumulation. This "morphing the distribution function" technique is not restricted to DLM VDFs. It would work as well with any non-Maxwellian VDF f_{nM} by the construction of a set of intermediate VDFs including an adiabatic switch , which would lead from the easily computable VDF f_0 to $f_0 + (f_{nM} - f_0)$ as 1. Alternate criteria can be used to choose f_0, such as by holding fixed the mean square error between itself and f_{nM} or by insisting that it be a sum of Maxwellians with particle numbers, widths, and center locations to be optimized to fit the particular VDF. In Figure 1, the

frequencies and damping rates of EPWs are plotted vs k_{De} for $n = 2, 3, 4,$ and 5. The substantial reduction in damping rates is clearly visible. Note that the first-order perturbation theory results

$$\frac{\omega_{EPW}}{\omega_{pe}} = \sqrt{1 + 3\left(k_{De}\right)^2}$$

(15)

and

$$\frac{\nu_{EPW}}{\omega_{pe}} = -\frac{\pi}{4} \frac{n}{\left((3/n)\Gamma_e^3\right)} \frac{1}{\left(k_{De}\right)^3}$$

$$\exp-\left[\frac{1}{\left(\Gamma_e k_{De}\right)^n} + \frac{3n}{2\Gamma_e^n} \frac{1}{\left(k_{De}\right)^{n-2}}\right]$$

(16)

are inaccurate for $k_{De} > 0.3$ in the Maxwellian case
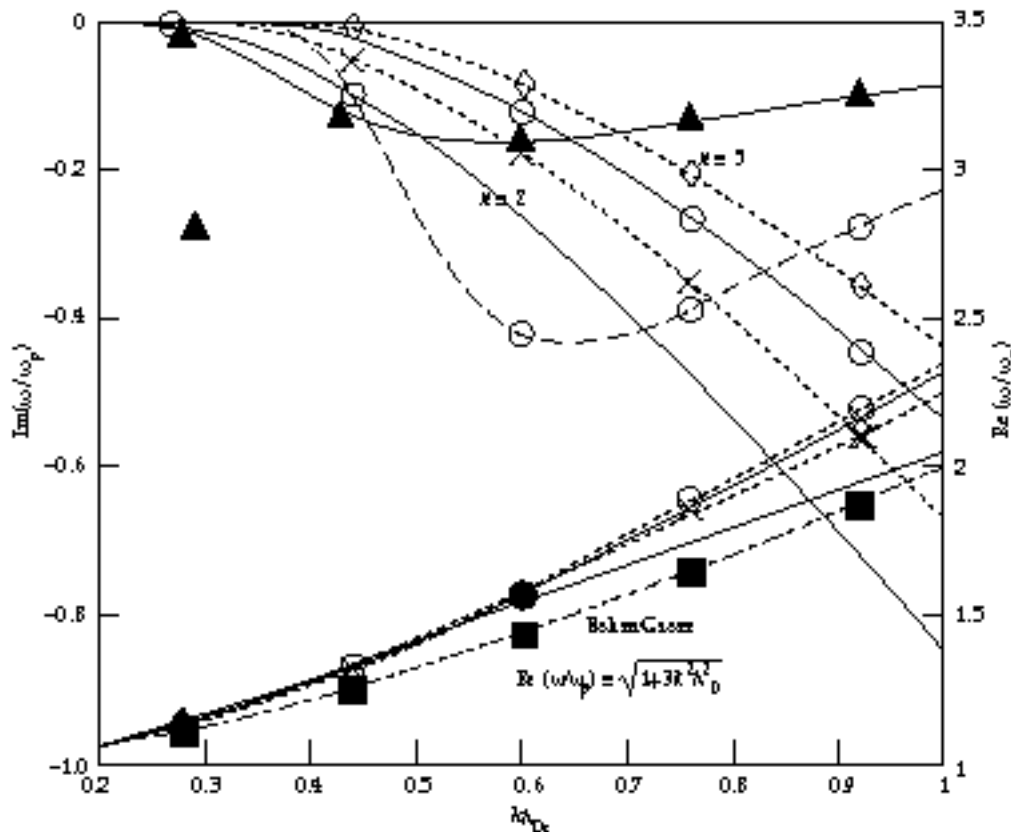

FIGURE 1. Frequencies and damping rates of EPWs in DLM VDFs normalized to the local plasma frequency ω_p vs k_{De}. The thick dashed curve is the analytic result for Landau damping of an EPW with $n = 5$, and the solid thick curve is the same for a Maxwellian ($n = 2$). The dotted curves with diamonds correspond to $n = 5$, the solid curves with open circles correspond to $n = 4$, the dotted curves with crosses correspond to $n = 3$, and the plain solid curves correspond to $n = 2$. The dot-dashed curve with filled squares is the Bohm–Gross frequency. (50-00-0797-1177pb01)

and much earlier for higher-n cases. For values of k_{De} of most interest in laser-plasma experiments today (0.2 to 0.5), the actual reduction in damping can be an order of magnitude and thus must be incorporated into any analysis of scattering data, as has been recently deduced.[12,13] In Figure 2, the damping rate of EPWs is plotted vs n for different values of k_{De}. In Figure 3, the damping rate of plasma waves in high-Z plasmas is given vs the relevant laser-plasma parameters. This figure shows that in a speckled laser beam, where hot spots can have 5× the average intensity, the modified distribution functions will reduce the threshold for high-frequency parametric instabilities precipitously. Note, too, that the usual Bohm–Gross frequency, as given in Eq. (9), can be in error by as
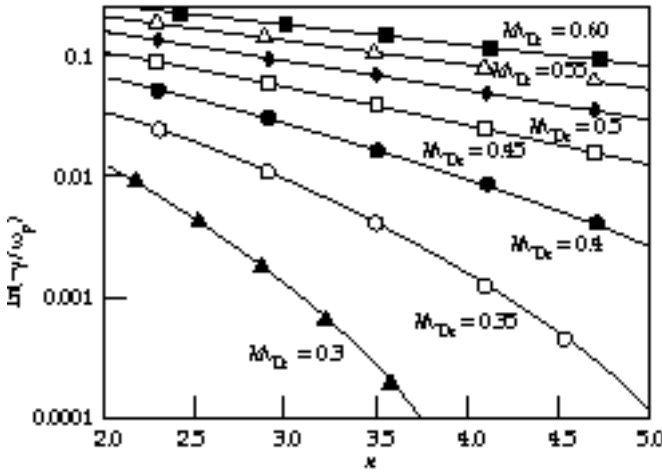

FIGURE 2. Damping rates of plasma waves in DLM VDFs normalized to the local plasma frequency ω_p vs the DLM exponent n for values of k_{De} ranging from 0.3 to 0.6 in steps of .05.   (50-00-0897-1603pb01)
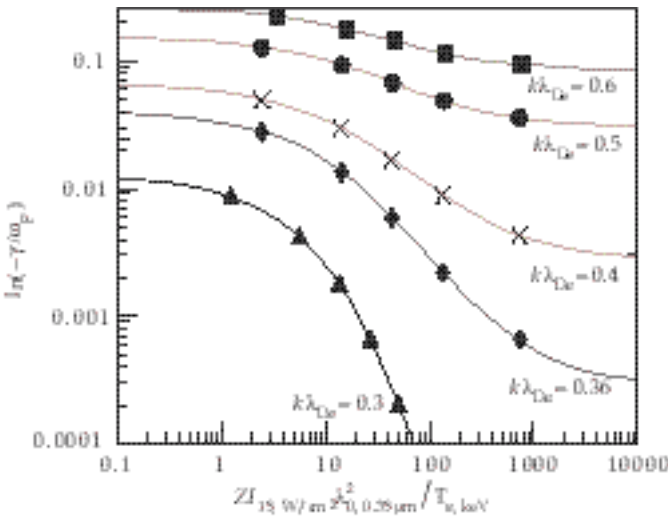

FIGURE 3. Damping decrement of electron–plasma waves normalized to the local plasma frequency ω_p vs $ZI_{15,W/cm^2}\lambda^2_{0,0.35\mu m}/T_{e,keV}$ for various values of k_{De}.   (50-00-0797-1178pb01)

In contrast, IAWs in high-Z plasmas will not have as dramatic a reduction in their damping rates. Instead, it is easily shown that their real frequencies increase with n by roughly twenty percent. The reason for this is the reduced number of cold electrons in higher-n distributions and the concomitant reduction in shielding available to the ions. This is the physical explanation for the parameter A defined in Eqs. (6) and (11). The renormalized sound speed (or the square root of the effective electron temperature) is given by the factor

$$C_{eff} = \sqrt{3\Gamma^2(3/n)/\left[\Gamma(1/n)\Gamma(5/n)\right]} \quad . \tag{17}$$

IAWs in such plasmas will have variable frequencies for the same k as they go in and out of laser hot spots and inhomogeneities of the illumination. This constitutes an additional source of dephasing for SBS, especially if the scattered light is traveling at a large angle with respect to the axes of the speckles. The perturbation theory result for the complex IAW frequency is

$$\omega_{IAW} = C_{eff}c_s k\left[\frac{1}{1+C_{eff}^2 k^2 \lambda_{De}^2} + 3\frac{T_i}{ZT_e}\right]^{1/2}, \tag{18}$$

and

$$\frac{v_{IAW}}{\omega_{IAW}} = -\sqrt{\frac{\pi}{8}}\left[\frac{\sqrt{2}C_{eff}}{\Gamma_e C_0}\left(\frac{Zm_e}{M_I}\right)^{1/2} + \frac{C_{eff}^3(ZT_e/T_i)^{3/2}}{\left[1+C_{eff}^2 K^2 \lambda_{De}^2\right]^{3/2}}\right.$$

$$\left. \times \exp\left(-\frac{C_{eff}^2(ZT_e/2T_i)^{3/2}}{\left[1+C_{eff}^2 K^2 \lambda_{De}^2\right]}\right)\right] \tag{19}$$

where $C_0 = 2\Gamma(1/n)/\left(n\sqrt{\pi}\right)$, $T_{e,i}$ is the electron/ion temperature, Z is the charge state, c_s is the ion acoustic speed, and $c_s^2 = ZT_e/M_i$. These are compared to the numerical solutions of the IAW dispersion relation in Figures 4 to 6 for different values of the wave number of the ion acoustic wave and different electron to ion temperature ratios.

The effect of changing the sound speed as a function of local laser intensity should be included in convective gain calculations for SBS that take into account flow inhomogeneities and laser nonuniformities.[30] For damping rates of the order of 0.1× the ion-acoustic
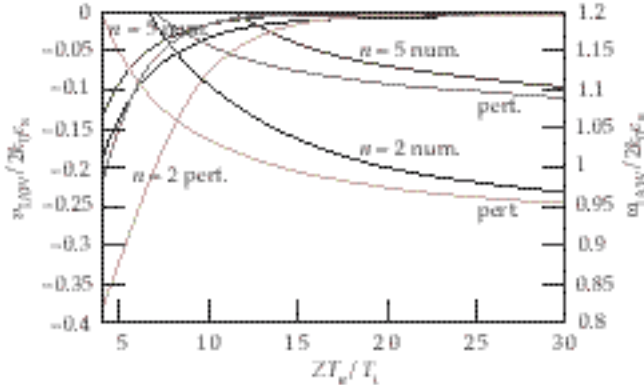
FIGURE 4. Frequencies and damping rates of IAWs in DLM electron and Maxwellian ion VDFs vs ZT_e/T_i for $k = 2k_0$. The $n = 2$ and $n = 5$ cases are plotted together with the results of perturbation theory as given in Eqs. (18) and (19). (50-00-0797-1179pb01)
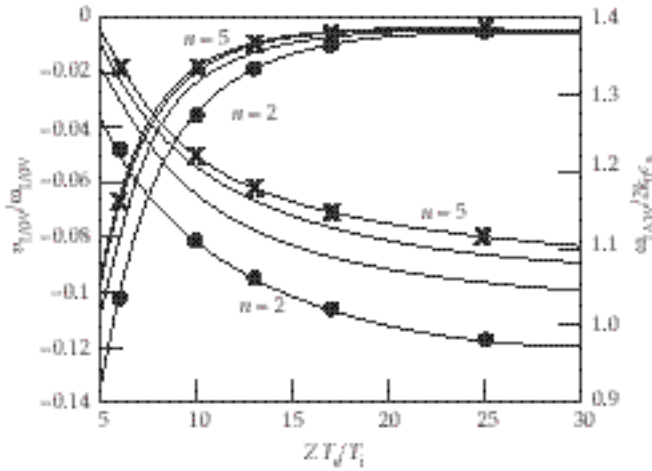

FIGURE 5. Frequencies and damping rates of IAWs in DLM electron and Maxwellian ion VDFs vs ZT_e/T_i for $k = 2k_0$. The $n = 2$, 3, 4 and 5 cases are shown. (50-00-0897-1602pb01)
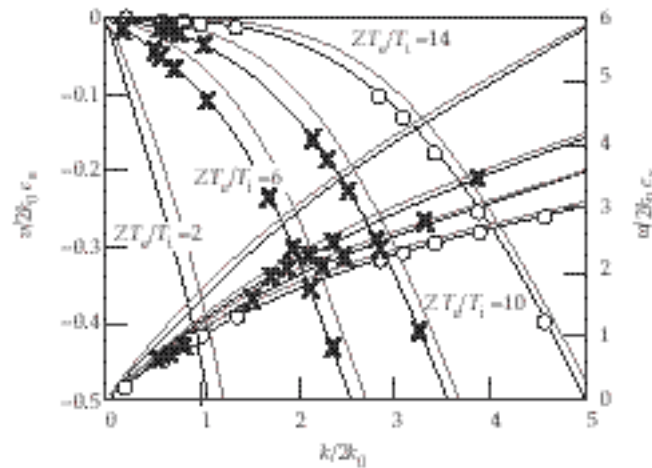

FIGURE 6. Frequencies and damping rates of IAWs in DLM electron and Maxwellian ion VDFs vs $k/2k_0$. $ZT_e/T_i = 2$, 6, 10 and 14 are plotted together with the approximate expressions given in Eqs. (18) and (19). (50-00-0897-1601pb01)

frequency, velocity fluctuations of order 10 to 20% have been shown to significantly reduce the gain of SBS.[31,30] The intensity-dependent frequency shift causes an additional reduction of the same order, while the angular dependence of this term is independent of and very different from that of the background flow profile. These effects help explain the low crossed beam gains observed in recent Nova experiments.[32,30]

Similar considerations for Raman lead to the picture that intensity-dependent *damping rates* will dictate the angular dependence of Raman gain. The reduction in damping inside hot spots will favor backscattered waves over side, and the ratio of the gain inside and outside hot spots can be many orders of magnitude, with pump depletion levels easily reached inside a single hot spot with only moderate gain outside. To show this, we use a typical $f/4$ hot spot and calculate the SRS gain as a function of angle for a gain length given by the length of the $I = 5I_{ave}$ region. The integrated reflectivity as a function of angle is given by the expression[15,30]

$$|a_s(L/2)|^2 = 1/L \int_{-L/2}^{L/2} d\theta \, |a_s(-L/2, \theta)| \exp[G(\theta)] \quad (20)$$

$$G(\theta) = 2 \left[\int_{-L/2}^{L/2} k(\theta, \zeta) d\zeta \right] \quad (21)$$

$$k_i(\text{SRS}) = -\frac{1}{2} \left[\frac{D_-}{k_{-//}} + \frac{D_s}{k_s} \right] +$$

$$\sqrt{\frac{1}{4} \left[\frac{D_-}{k_{-//}} + \frac{D_s}{k_s} \right]^2 + \frac{\omega_0^2}{4k_{-//} k_s}} \quad (22)$$

where ζ is the direction along the scattered Raman beam and θ is perpendicular to it, the component of the wave vector of the EPW along the scattered light direction is $k_{-//} = \sqrt{\varepsilon} \cos\theta_s - k_s$, the k vector magnitude of the scattered light wave is

$$k_s = \pm \sqrt{1 - 2\sqrt{\frac{n/n_c + 5.87 \times 10^{-3} T_{e,keV}}{\times \varepsilon - 2\sqrt{\varepsilon} k_s^0 \cos\theta_s + k_s^{(0)2}}}} \quad ,$$

θ_s is the angle between the pump and scattered light k vectors, $k_s^{(0)} = k_s(T_{e,keV} = 0)$, $\varepsilon = 1 - n/n_c$, the dispersion relation of the EPW is

$$D_- = \left[(\omega_0 - \omega_s)v_{EPW}\right]/\omega_0^2 + (i/2)\left[(\omega_0 - \omega_s)\nu/\omega_0^2 - V_n\right],$$

the frequency of the EPW beyond the Bohm–Gross frequency is ω, the dispersion relation for the scattered light wave is $D_s = \left[v_s/\omega_s\right]\left[n/n_c\right] + i/2V_n$, and potential density inhomogeneities and fluctuations are given by

$$V_n = \left[\omega_p^2(\cdot,\cdot) - \omega_p^2(0)\right]/\omega_0^2, \text{ and}$$

$$\kappa_0^2 = (1/4)(v_0^2/c^2)(n/n_c) k_-^2.$$

In Figure 7, we plot the gain of SRS as a function of angle for CH, Ti, and Xe, where $\bar{Z} \equiv \langle Z^2\rangle/\langle Z\rangle = 5$, 21, and 40 respectively, the electron temperature in the plasma $T_e = 3$ keV, the laser wavelength $\lambda_0 = 0.35\,\mu$m, and the average laser intensity $I_{ave} = 10^{15}$ W/cm^2. The gain exponent for straight backscatter through the

FIGURE 7. $G^{(SRS)}$ vs near-backscattering angles for $T_e = 3$ keV, $I_{ave} = 10^{15}$ W/cm^2, $n/n_c = 0.1$, and (a) $\bar{Z} = 40$ (solid line, and dashed line in the case of fixed damping at the average intensity); (b) $\bar{Z} = 21$ (solid line with x's, and dashed line with x's in the case of fixed damping at the average intensity); (c) $\bar{Z} = 5$ (solid line with circles) and dashed line with circles in the case of fixed damping at the average intensity).   (50-00-0797-1180pb01)

center of the hot spot where $I > 5I_{ave}$ is ~32 in the case of CH with a density of $0.1n_c$. This is consistent with very strongly collimated SRS emission, which has been observed in recent Nova experiments.[11] The effect for higher-Z materials is even more dramatic, and suggests the picture that steep-temperature-gradient–driven transport off the sides of an intense hot spot, which gives rise to depleted-tail VDFs,[9] will produce electron–plasma waves with significantly lower Landau damping and therefore larger Raman scattering in the hot spot. Large-amplitude plasma waves will be created by SRS inside the hot spots as the instability saturates, and large density and velocity fluctuations will remain in their wake. While quantitative numerical studies are needed to confirm the range of validity of the following scenario, it is hypothesized that such SRS-dominated hot spots will not be amenable to significant SBS growth even in the saturated SRS regime. When these fluctuations have dissipated their energy at typically ion-acoustic transit or ion–ion collision time scales, SRS will return, and the cycle will repeat itself. This model implies that in moderate- to high-Z plasmas with RPP beams, SRS will dominate the hot spots while SBS is forced to occur well outside these regions of highest intensity.

Nonlocal heat transport and vigorous bremsstrahlung heating-modified distribution functions, which as a class are well captured by the DLM VDFs, can play an important role in determining when SRS dominates hot spots and how low in density one must go before SRS is turned off so that SBS can take advantage of hot-spot intensities and grow to larger levels. In fact, a recent experiment by Montgomery[17] has shown that the SBS gain increases by two orders of magnitude in a CH plasma when the density is reduced from $0.1n_c$ to $0.07n_c$. The relative levels of Raman and Brillouin reflectivity measured in that experiment as a function of density are consistent with the picture that at the lower density, Raman is not strong enough to dominate the hot spots, and that Brillouin occurring in hot spots with five times the average intensity overcomes the reduction due to a decrease in density and produces the two orders of magnitude increase in SBS reflectivities seen experimentally. In order to investigate further the hot-electron dynamics and instability development in the presence of nonlocal heat transport and steep temperature gradients in moderate- to high-Z materials, Fokker–Planck transport calculations are required in conjunction with parametric instability models. We hope to address this challenging problem next.[33]
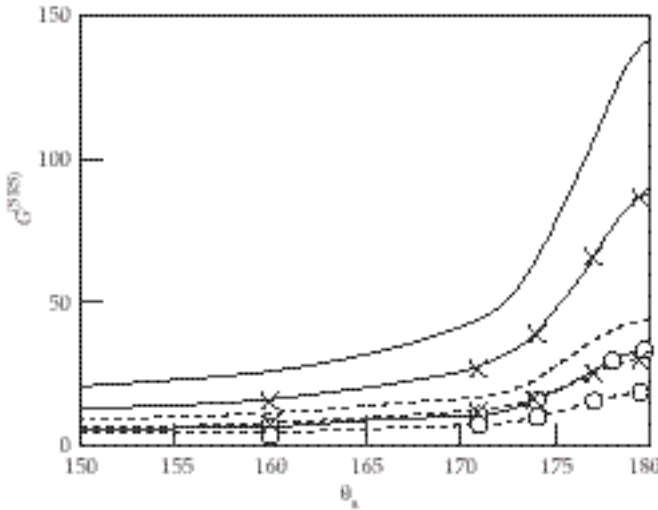
Summary

In high-Z plasmas, or in laser hot spots with moderate Z, the damping rate of an electron-plasma wave (EPW) is substantially lower and the frequency of an ion-acoustic wave (IAW) significantly higher than those in a Maxwellian distribution. EPWs and IAWs were analyzed in flat-topped and depleted-tail electron velocity distribution functions that arise due to nonlocal heat transport and vigorous bremsstrahlung heating in high-intensity lasers. In such plasmas, SRS can dominate the most intense laser hot spots, excluding SBS from such hot spots unless the density is low enough to eliminate SRS.

Acknowledgments

Notes and References

1. R. Z. Sagdeev and A. A. Galeev, *Non-Linear Theory of Plasma*, Benjamin, New York, N. Y., 1969.
2. C. T. Dum, *Phys. Fluids* **21**, 945–956 (1978).
3. A. B. Langdon, *Phys. Rev. Lett.* **44**, 575 (1980).
4. R. D. Jones and K. Lee, *Phys. Fluids* **25**, 2307 (1982).
5. P. Alaterre, J. P. Matte, and M. Lamourex, *Phys. Rev. A* **34**, 1578 (1986).
6. J. P. Matte et al., *Plasma Phys. Cont. Fusion* **30**, 1665 (1988).
7. J. M. Liu et al., *Phys. Plasmas* **1**, 3570 (1994).
8. P. Mora, *Phys. Rev. A* **26**, 2259 (1982).
9. J. A. Albritton, *Phys. Rev. Lett.* **50**, 2078 (1983) and **57**, 1887 (1986).
10. T. J. Orzechowski et al., *Bull. Amer. Phys. Soc.*, 1996.
11. B. J. MacGowan et al., *Phys. Plasmas* **3**, 2029 (1996).
12. R. K. Kirkwood et al., *Phys. Rev. Lett.* **77**, 2706 (1996).
13. J. C. Fernandez et al., *Phys. Rev. Lett.* **77**, 2702 (1996).
14. W. L. Kruer, "*The Physics of Laser-Plasma Interactions*," *Frontiers in Physics* series, No. 73, Addison-Wesley Publishing Co., 1988.
15. C. S. Liu, in *Advances in Plasma Physics*, Vol. 16, ed. A. Simon and W. Thompson, J. Wiley & Sons, New York, N. Y., 1976.
16. H. A. Baldis, E. M. Campbell, and W. L. Kruer, in *Handbook of Plasma Physics*, Vol. 3, ed. A. Rubenchik and S. Witkowski, North-Holland, N. Y., 1991.
17. D. S. Montgomery et al., submitted to *Phys. Rev. Lett.* (1996).
18. S. J. Karttunen, *Phys. Rev. A* **23**, 2006 (1981); J. A. Heikkinen and S. J. Karttunen, *Phys. Fluids* **29**, 1291 (1986).
19. B. Bezzerides, D. F. Dubois, and H. A. Rose, *Phys. Rev. Lett.* **70**, 2569 (1993).
20. T. Kolber, W. Rozmus, and V. T. Tikhonchuk, *Phys. Fluids B* **5**, 138 (1993).
21. K. L. Baker, Ph. D. dissertation, University of California at Davis (1996).
22. R. P. Drake et al., *Phys. Fluids* **31**, 1795 (1988); R. P. Drake et al., *Phys. Fluids B* **1**, 2217 (1989).
23. C. Rousseaux et al., *Phys. Fluids B* **5**, 920 (1993).
24. V. Yu. Bychenlov et al., *Phys. Plasmas* **4**, 1481 (1997); J. Zheng et al., *Phys. Plasmas* **4**, 2736 (1997).
25. S. M. Dixit et al., *Appl. Optics* **32**, 2543 (1993).
26. J. F. Drake et al., *Phys. Fluids* **17**, 778 (1974).
27. S. C. Wilks et al., *Phys. Fluids B* **4**, 778 (1992).
28. W. Seka et al., *Phys. Fluids* **27**, 2181 (1984).
29. D. S. Montgomery et al., *Phys. Plasmas* **3**, 1728 (1996).
30. B. B. Afeyan et al., submitted to *Phys. Plasmas* (1997).
31. W. L. Kruer et al., *Phys. Plasmas* **3**, 382 (1995).
32. R. K. Kirkwood et al., *Phys, Rev. Lett.* **76**, 2065 (1996).
33. B. B. Afeyan et al., submitted to *Phys. Rev. Lett.* (1997).